Journal of Atmospheric Chemistry **44:** 225–240, 2003.

Impact of Accurate Photolysis Calculations on the Simulation of Stratospheric Chemistry

JÖRG TRENTMANN [1], HEINRICH BOVENSMANN [2⋆], VERONIKA EYRING [2, 3], RICHARD W. MÜLLER [2, 4] and JOHN P. BURROWS [2]

[1] *Max Planck Institute for Chemistry, Biogeochemistry Dept., PO Box 3060, D-55020 Mainz, Germany, e-mail: jtrent@mpch-mainz.mpg.de*
[2] *Institute for Environmental Physics, University of Bremen, PO Box 330440, D-28334 Bremen, Germany, e-mail: bov@iup.physik.uni-bremen.de*
[3] *DLR-Institut für Physik der Atmosphäre, Oberpfaffenhofen, D-82234 Wessling, Germany*
[4] *Carl-von-Ossietzky Universität Oldenburg, EHF, Fachbereich Physik, Carl-von-Ossietzky Str. 9–11, D-26129 Oldenburg, Germany*

(Received: 30 March 2001; in final form: 11 July 2002)

Abstract. The interpretation of atmospheric measurements and the forecasting of the atmospheric composition require a hierarchy of accurate chemical transport and global circulation models. Here, the results of studies using *Bremens Atmospheric Photochemical Model* (BRAPHO) are presented. The focus of this study is given to the calculation of the atmospheric photolysis frequencies. It is shown that the spectral high resolved simulation of the O_2 Schumann–Runge bands leads to differences in the order of 10% in the calculated O_2 photolysis frequency when compared with parameterizations used in other atmospheric models. Detailed treatment of the NO absorption leads to even larger differences (in the order of 50%) compared to standard parameterizations. Refraction leads to a significant increase in the photolysis frequencies at large solar zenith angles and, under polar spring conditions, to a significant change in the nighttime mixing ratio of some trace gases, e.g., NO_3. It appears that recent changes in some important rate constants significantly alter the simulated BrO_x- and HO_x-budgets in the mid-latitude stratosphere.

Key words: photochemical boxmodel, photolysis frequency, radiative transfer, stratospheric chemistry.

1. Introduction

Stratospheric photochemical models are widely used for the interpretation of atmospheric measurements and the forecasting of the atmospheric composition (Ravishankara *et al.*, 1999, and references therein). Although significant efforts have been done in the development of these models, there still remain a lot of open questions when comparing model results with measurements.

⋆ Corresponding author.

Chemical transport models underestimate the ozone loss during polar spring as compared to observations especially in the Arctic (Hansen *et al.*, 1997; Becker *et al.*, 2000b; Woyke *et al.*, 1999). A 2-dimensional model study reveals an overestimation of the NO_y concentration in the upper stratosphere (Nevison *et al.*, 1997). Balloon borne NO_3 measurements show a disagreement between measurements and model results in the lower stratosphere (Renard *et al.*, 1996). The observed peak in the HO_x concentration during sunrise near the tropopause is not yet satisfactory explained by model studies (Salawitch *et al.*, 1994; Wennberg *et al.*, 1999). For many of these unanswered questions, photolysis frequencies are critical model parameters. Therefore, a detailed knowledge of the atmospheric radiative transfer and accurate calculation of the photolysis rates are necessary to evaluate stratospheric models. Recently, it was demonstrated that an improved numerical solution of a widely used photolysis scheme (Lary and Pyle, 1991) is affecting stratospheric photolysis rates significantly (Becker *et al.*, 2000a).

In this study, model results of the photochemical box model BRAPHO (Bremens Atmospheric Photochemical Model) that includes sophisticated calculation of atmospheric photolysis frequencies are presented. BRAPHO includes the model PHOTOGT (Blindauer *et al.*, 1996) for the calculation of the photolysis frequencies. In Section 3, an investigation of the photolysis frequencies of O_2 and NO are presented and compared with results from other radiative transfer models. Differences arise as a results of the assumptions with respect to the spectrally highly varying cross sections of O_2 and NO. The impact of refraction on the photolysis frequencies at large solar zenith angle (SZA) and photochemistry is discussed in Section 4. In Section 5, the impact of new absorption cross section of HOBr in combination with a new recommendation for heterogeneous $BrONO_2$ hydrolysis on stratospheric chemistry is presented.

2. BRemens Atmospheric PHOtochemical model (BRAPHO)

In this section, the different modules of BRAPHO are described. BRAPHO has already been used successfully for stratospheric studies including the simulation of the diurnal cycle of polar ClO (Raffalski *et al.*, 1998), the identification of stratospheric IO (Wittrock *et al.*, 2000) and the interpretation of the mid-stratospheric ozone variability (Sinnhuber *et al.*, 1999), but its details have not been previously described. Additionally, it participated successfully in an intercomparison between German stratospheric chemical models (Krämer *et al.*, 2002).

2.1. PHOTOLYSIS FREQUENCIES

The photolysis frequency of an atmospheric molecule, J, is calculated as the wavelength integral over the product of actinic flux, the absorption cross section, and the quantum yield of the molecule (Madronich, 1987).

Within BRAPHO photolysis frequencies are calculated with PHOTOGT (PHOTOGOMETRAN). Details of PHOTOGT were presented in Blindauer *et al.* (1996). Therefore we only briefly summarize the main features of the model.

To calculate the intensity of the diffuse solar light, the pseudospherical version of the one-dimensional radiative transfer model GOMETRAN is used (Rozanov *et al.*, 1997). It solves the radiative transfer equation using the 'finite difference method'. The actinic flux is calculated by adding the direct and the surface-reflected beam to the diffuse light (Blindauer *et al.*, 1996). Refraction is taken into account for the direct beam. The implementation of refraction is based on the variation of the refractive index of the air with height and described in Eichmann (1995). The calculation of the actinic flux is performed on different wavelength intervals ranging from 0.5 cm^{-1} ($\approx$0.002 nm) to 20 cm^{-1} ($\approx$0.5 nm) between 175 nm and 850 nm. Recently, GOMETRAN has been extended to SCIATRAN by the inclusion of line-by-line and correlated-k coefficients to describe line absorbers (Buchwitz *et al.*, 2000). The molecular parameters – absorption cross section and quantum yield – are taken from compilations (DeMore *et al.*, 1997; Atkinson *et al.*, 1997). Integration over the wavelength is performed using Simpson's rule (Press *et al.*, 1992). For the use within BRAPHO, the calculated photolysis frequencies for the specified atmospheric profiles are stored in look-up tables at certain SZAs (ΔSZA $\approx$ 0.5–2°) and linearly interpolated in between.

The structure of PHOTOGT allows the easy implementation of updated or new molecular parameters to calculate the photolysis frequency.

2.1.1. *Treatment of the O_2 Schumann–Runge Bands*

Light absorption of molecular oxygen plays a decisive role in stratospheric chemistry. Absorption of O_2 strongly influences the attenuation of solar light; photodissociation of molecular oxygen provides the only source of stratospheric ozone.

The absorption cross section of O_2 in the Schumann–Runge bands between 175 and 205 nm shown in Figure 1 is highly spectrally structured and temperature dependent. In PHOTOGT, the calculation of the actinic flux and the O_2 photolysis frequency is performed using the temperature dependent spectral high resolved (0.5 cm^{-1}) cross sections from Minschwaner *et al.* (1992) in the Schumann–Runge bands. For the underlying Herzberg continuum (185–242 nm) the cross sections of Yoshino *et al.* (1988) are used. The validation of the actinic flux calculation can be found in Blindauer *et al.* (1996). A comparison of photolysis frequencies of O_2 and NO calculated using the high spectral resolved cross sections with simplified broadband parameterizations are discussed in Section 3. Other species that dissociate in this wavelength region include N_2O and H_2O. While photolysis of N_2O in the stratosphere is the main atmospheric sink for nitrogen oxide (Minschwaner *et al.*, 1993; Prather *et al.*, 2001), photodissociation of H_2O is an important source for HO_x radicals in the mesosphere (Siskind *et al.*, 1994). The calculation of their

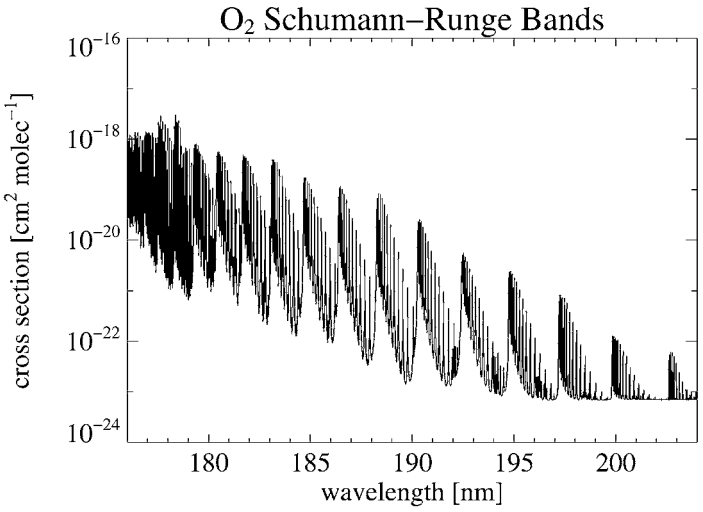

Figure 1. Absorption cross section of O_2 in the Schumann–Runge bands at 216 K (Minschwaner *et al.*, 1992).

photolysis frequencies is also affected by the simulation of the radiative transfer in the wavelength region of the O_2 Schumann–Runge bands.

2.1.2. *Calculation of the NO Photolysis Frequency*

Photodissociation of nitric oxide (NO) occurs in two absorption bands in the UV wavelength region where the actinic flux is determined by the O_2 absorption in the Schumann–Runge bands.

Similar to the O_2 Schumann–Runge bands, the absorption cross section of NO is highly structured and temperature dependent. In Figure 2 the NO absorption cross section in the $\delta(1, 0)$ band (181.49 nm–183.49 nm) from Minschwaner and Siskind (1993) are shown. To calculate the NO photolysis frequency also the $\delta(0, 0)$ band (189.39 nm–191.57 nm) which shows a similar spectral structure is included. Other absorption bands only have a 1% effect on the photolysis frequency and are therefore negligible (Minschwaner and Siskind, 1993). Also shown in the figure are the O_2 cross sections in this wavelength region (scaled with a factor of 10^{-5}). The spectral variation of the NO cross sections is even an order of magnitude larger than for the O_2 cross section, 0.05 cm^{-1} and 0.5 cm^{-1}, respectively.

Within PHOTOGT these highly spectrally resolved temperature dependent cross sections are used to calculate J(NO). The actinic flux is calculated on the spectral grid of the O_2 cross sections and interpolated onto the grid of the NO cross sections.

The significant differences which are induced using simplified, broadband parameterizations to calculate the NO photolysis frequency compared to the accurate calculation of PHOTOGT are discussed in Section 3.2.

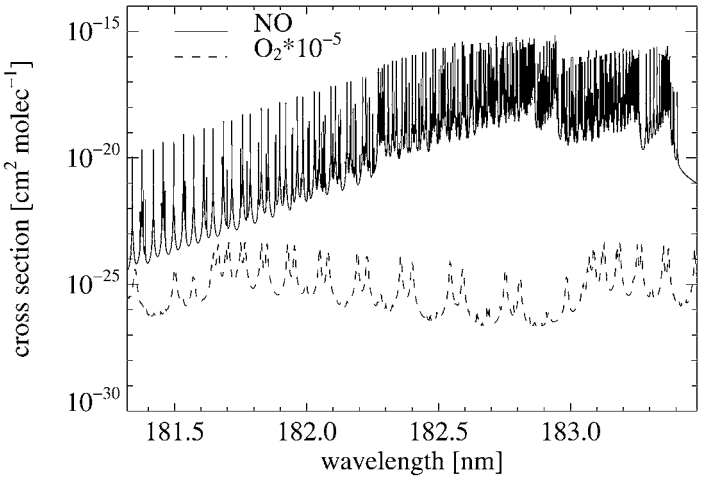

Figure 2. Spectral resolved absorption cross section of NO at 216 K, $\delta(1, 0)$ band (Minschwaner and Siskind, 1993). For comparison the O_2 cross sections (scaled with a factor 10^{-5}) in this wavelength region are also shown (Minschwaner *et al.*, 1992) (figure after Minschwaner and Siskind (1993)).

2.2. HETEROGENEOUS REACTIONS

BRAPHO includes heterogeneous reactions on liquid and solid aerosols as well as on ice particles. The reaction rates are calculated using a model developed at the Max Planck Institute for Chemistry, Mainz, Germany, by K. Carslaw. This module calculates the volume and the composition of the liquid aerosol particles from the temperature, pressure, and the gas phase concentrations of H_2SO_4, H_2O, and HNO_3 using an analytical formula (Carslaw *et al.*, 1995). Uptake of HCl, HOCl, and HBr changes the gas phase concentrations as well as the composition of the aerosol. The uptake coefficients and reaction rates are calculated using the formulas derived by Hanson *et al.* (1994) based on the recommendations of DeMore *et al.* (1997).

Additionally, different pathways for phase transitions (melting, freezing) can be chosen according to Peter (1997). These include, e.g., the three-stage concept (Poole and McCormick, 1988) as well as the possibility of the existence of liquid particles down to the ice freezing temperature (Koop *et al.*, 1995). NAT, SAT and ice particles are treated in equilibrium using the formulation of Hanson and Mauersberger (1988) (NAT, ice) and Tabazadeh *et al.* (1994) (SAT). The reaction rates are calculated using the formula given in Hanson *et al.* (1994) using sticking coefficients based on the recommendations of DeMore *et al.* (1997). More detailed information on the treatment of heterogeneous processes within BRAPHO can be found in Eyring (1999).

2.3. CHEMICAL REACTION SCHEME AND NUMERICAL SOLUTION

The selection of the chemical reactions is based on the Mainz Box Model (Crutzen *et al.*, 1992; Grooß *et al.*, 1997) which includes O_x, NO_x, HO_x, Cl_x, Br_x and methane chemistry. The evolution of 39 chemical compounds is simulated taking into account 127 chemical reactions (77 bimolecular, 9 trimolecular, 4 thermal decomposition, 26 photolysis, and 11 heterogeneous reactions). The reaction rate constants, absorption cross sections and quantum yields are mostly taken from DeMore *et al.* (1997). The most important exceptions are the absorption cross sections of O_2 and NO which are described in more detail than recommended by DeMore *et al.* (1997).

The transformation of the selected chemical reactions to a differential equation system as well as the numerical integration of this system is performed using the ASAD (A Self-contained Atmospheric chemistry coDe) package (Carver *et al.*, 1997). It allows the user to choose between different methods to solve the stiff differential equations with different complexity. Within BRAPHO, the SVODE integrator is used which is based on the Backward Differential Formula (BDF) (Brown *et al.*, 1989). This method explicit calculates the concentrations of the different species without making use of the family concept.

3. Impact of Parameterizations on Photolysis Frequency Calculations

3.1. O_2 PHOTOLYSIS FREQUENCY

In the following section, the photolysis frequency of molecular oxygen calculated with different parameterizations of the O_2 Schumann–Runge absorption bands are compared with results from PHOTOGT. One very common parameterization is the one from Allen and Frederick (1982) (A&F) which is recommended in WMO (1985) and also includes the Herzberg continuum (185–242 nm). Another parameterization of the Schumann–Runge bands is based on the opacity distribution functions (ODFs) (Minschwaner *et al.*, 1993; Siskind *et al.*, 1994). An improved version of the ODFs including the temperature dependency of the cross sections (ODF-T) is also in use (Prather, 1993). However, neither of these approaches incorporated the full information of the spectral high resolved O_2 absorption cross section in the radiative transfer simulations leading to less accurate results (Minschwaner *et al.*, 1993).

The O_2 photolysis frequency calculations using these parameterizations are taken from the NASA Photolysis Rate Intercomparison for Assessment Models (Stolarski, 1995). The DISORT model (Dahlback and Stamnes, 1991) uses the standard ODFs while the UCI model (Prather, 1993) uses the improved ODFs (ODF-T). The model of the CSIRO (Randeniya *et al.*, 1996) uses the parameterization of A&F. For the calculations with PHOTOGT the same atmospheric scenario (temperature and ozone profile, ground albedo) as in the NASA intercomparison assessment was used (R. Kawa, pers. communication).

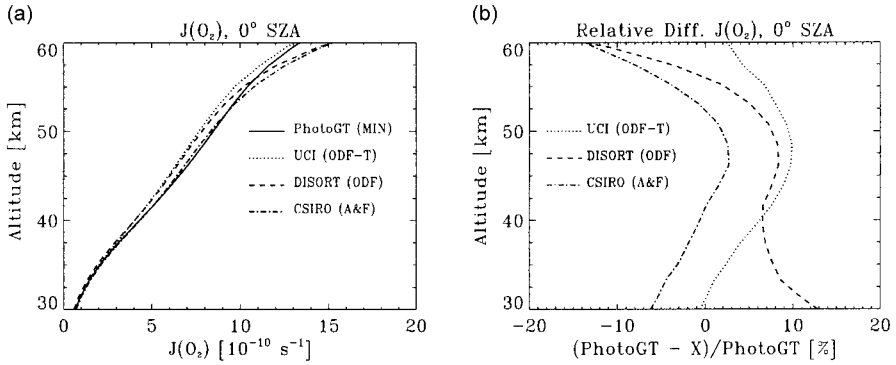

Figure 3. (a) O_2 Photolysis frequencies calculated with different models using different parameterizations of the Schumann–Runge bands (see text for details); (b) relative difference between PHOTOGT and the other models.

In the wavelength region of the O_2 photolysis, the actinic flux is determined by absorption while scattering is only of minor importance. As the absorption is treated identically in all models no significant difference arises from the different model formulations, especially at low SZA.

In Figure 3 the photolysis frequency of O_2 calculated with the different parameterizations and the relative differences to the calculation with PHOTOGT at 0° SZA between 30 and 60 km altitude are shown. The relative differences are in the range of 10% for overhead sun. This is consistent with the results of Siskind *et al.* (1994) and Koppers and Murtagh (1996). For larger SZAs, the differences increase up to ±30% (for 90° SZA, not shown), with CSIRO (A&F) and UCI (ODF-T) overestimating and DISORT (ODF) underestimating $J(O_2)$.

For stratospheric photochemistry this difference has significant influence on ozone production. As the correct calculation of the O_2 photolysis frequency is crucial to examine the ozone budget in the upper atmosphere, care has to be taken when addressing this question using parameterization for the calculation of $J(O_2)$ (Grooß *et al.*, 1999).

3.2. NO PHOTOLYSIS FREQUENCY

Similar to the absorption spectrum of O_2 in the Schumann–Runge bands there also exist parameterizations of the temperature dependent NO cross sections. The first parameterization was introduced by Allen and Frederick (1982) (A&F). Similar to the oxygen spectrum there are also ODFs (Minschwaner and Siskind, 1993) which were calculated from temperature dependent spectral high resolution cross sections. In PHOTOGT the high resolution cross sections shown in Figure 2 are used. In Figure 4 the simulated NO photolysis frequencies and the relative differences to the PHOTOGT calculations are shown for the same models as in Section 3.1. There are two reasons for the differences in the calculated NO photolysis frequency: first,

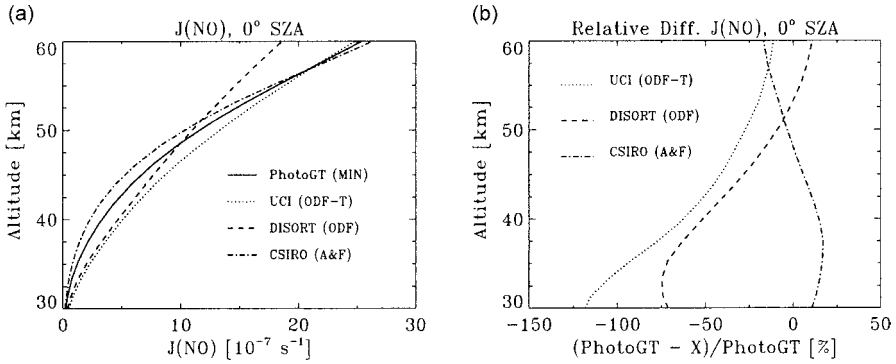

Figure 4. (a) NO photolysis frequencies at 0° SZA calculated with different models and different parameterizations for the Schumann–Runge bands and the NO cross sections (see text for details); (b) relative difference between PHOTOGT and the other models.

the different treatment of the Schumann–Runge bands of oxygen (Section 3.1) leads to differences in the actinic flux. Second, the use of different parameterization for the NO cross sections as described above lead to additional differences. The CSIRO model uses the A&F parameterization for the Schumann–Runge bands and for the NO cross sections. DISORT and the UCI model use both the ODFs for the NO cross sections, but differ in the treatment of the Schumann–Runge bands as described in Section 3.1.

The relative differences in the calculated NO photolysis frequency exceed those of the O_2 photolysis frequency by far. They even increase at larger solar zenith angles and easily reach more than 100%. This large errors indicate that the simple approximations are poor descriptions of the NO photolysis in the upper atmosphere. This is important for atmospheric chemistry where NO photolysis is a significant process, e.g., in the upper stratosphere and mesosphere (Nevison *et al.*, 1997).

4. Influence of Refraction on Photochemistry

At large solar zenith angles (low sun) refraction leads to a significant increase in the actinic flux and the atmospheric photolysis frequencies (DeMajistre *et al.*, 1995).

In Figure 5 the relative difference of the photolysis frequencies of selected molecules which dissociate in different wavelength regions of the solar spectrum in 20 km altitude calculated including and neglecting refraction are shown. Below 90° SZA the difference is negligible (<1%), but reaches nearly 100% at large solar zenith angles. The largest difference is observed in the photolysis frequency of NO_3 which dissociates in the visible wavelength region where the contribution of the direct solar radiation, which is primarily affected by refraction, to the actinic flux is relatively large. At shorter wavelengths, higher Rayleigh scattering and absorption lead to much larger attenuation of the direct light at large SZA (long light

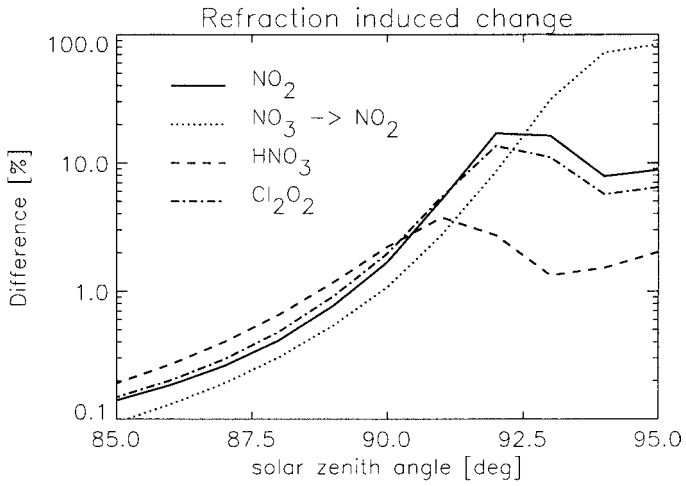

Figure 5. Relative difference of various photodissociation frequencies at 20 km between the simulations including and neglecting refraction.

path). Therefore the direct solar radiation contributes less to the actinic flux, and the impact of refraction is smaller. This is consistent with the findings of DeMajistre *et al.* (1995).

To asses the impact of refraction on polar stratospheric chemistry, BRAPHO is used to simulate atmospheric chemistry at 78.9° N (Ny Alesund, Spitzbergen) and 50 hPa (≈20 km) on 13 March 1997. Initial concentrations were taken from the 3 dimensional SLIMCAT CTM Model (Chipperfield, 1999) and show denitrification ($[NO_x] \approx 100$ ppt, $[NO_y] \approx 9$ ppb) and small chlorine activation ($[ClO_x] \approx 650$ ppt). The temperature was derived from ECMWF data and kept constant at 198 K. Model simulations were performed for two days, the presented results are taken from the second day. Two simulations are compared: one including and one neglecting refraction in the calculation of the photolysis frequencies.

As already mentioned by DeMajistre *et al.* (1995) and Balluch and Lary (1997) the effect of refraction on the simulated ozone concentration is negligible for short timescales. However, for the simulation of other trace gases refraction has to be taken into account. In Figure 6 the NO_3 mixing ratios for the two simulations are shown. A difference of nearly 100% during night is observed with lower values in the simulation including refraction. The higher NO_3 photolysis rate and especially the longer duration of NO_3 photolysis during sunset leads to increased NO_2 concentrations. Due to enhanced Cl_2O_2 photolysis (Figure 5) also more ClO is available. ClO and NO_2 react to form $ClONO_2$ which photodissociates at short wavelength. Therefore, the $ClONO_2$ photolysis is not significantly enhanced when refraction is taken into account and the nighttime $ClONO_2$ concentrations are enhanced in the simulations including refraction. Under these polar stratospheric conditions, refraction leads to a decrease in the nighttime NO_3 mixing ratio by nearly a factor of two. Therefore refraction has to be taken into account when

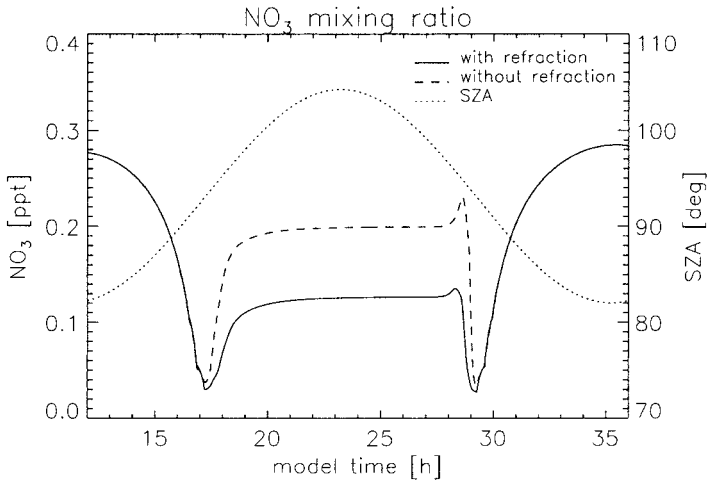

Figure 6. NO_3 mixing ratio for the polar scenario including and neglecting refraction. The dotted line represents the SZA (right scale).

comparing stratospheric NO_3 measurement with model calculations, especially for nighttime conditions, e.g., those presented by Renard *et al.* (1996).

5. Bromine Chemistry and Photolysis Frequencies

In this section, the impact of new absorption cross sections for HOBr (Ingham *et al.*, 1998) together with a new parameterization for the heterogeneous hydrolysis of bromine nitrate ($BrONO_2 + H_2O \longrightarrow HOBr + HNO_3$) on sulphate aerosols, both recommended in JPL 2000 (Sander *et al.*, 2000), is presented. The new HOBr absorption cross sections lead to a higher photolysis frequency of HOBr especially at large SZA (sunrise and sunset). The new rate constant for the heterogeneous hydrolysis of bromine nitrate is about a factor of 2 higher for typical stratospheric mid-latitude conditions in late winter.

For this study, BRAPHO is used as a box model to simulate mid-latitude stratospheric chemistry at 50 hPa (≈20 km) at Bremen, Germany (53° N, 4° E) on 4 March 1997. The temperature was taken from ECMWF data and set to T = 213 K. Initial concentrations were taken from the SLIMCAT model (Chipperfield, 1999) and represent typical mid-latitude late winter conditions. Model simulations were performed for two days, the presented results are taken from the second day. Two model runs were performed: One using the rate constants from the old recommendation (DeMore *et al.*, 1997) combined with temperature dependent heterogeneous reaction rates (Carslaw *et al.*, 1995) and another using the two updated rate constants from Sander *et al.* (2000).

Figure 7 shows the simulated daytime BrO mixing ratio of the two model configurations. Due to the combined effect of the increased heterogeneous production of HOBr during night and faster photolysis during sunrise, the morning BrO mixing

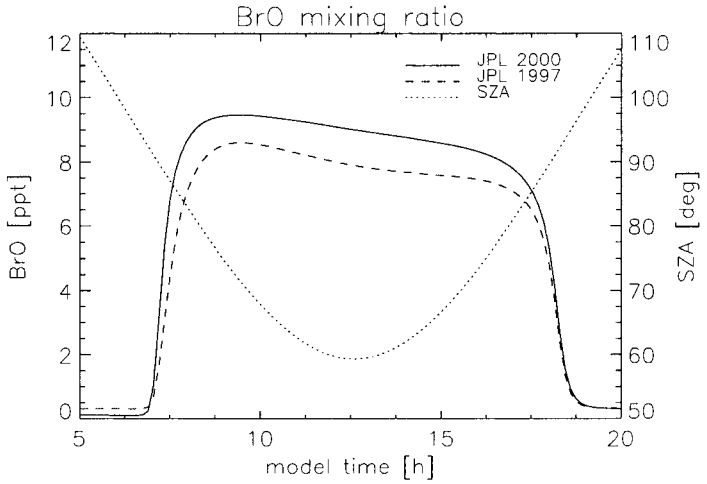

Figure 7. Simulated BrO mixing ratio of the simulations using the old recommendation (JPL 97, Carslaw *et al.*, 1995) and the 2 updated bromine reaction rates (JPL 2000). The dotted line represents the SZA (right scale).

ratio is significantly enhanced in the simulation using the new evaluation. These new laboratory data significantly improve the agreement between model simulations and BrO measurements in mid-latitudes at sunrise using the DOAS technique as shown by Müller *et al.* (2002).

In Figure 8 the simulated HO_x ($= OH + HO_2$) mixing ratios from the two model simulations are shown. Higher HOBr concentrations and faster HOBr photolysis in the morning lead to the local maximum in the HO_x concentration shortly after sunrise in the simulation using the data from the new evaluation.

Observations in the lower stratosphere show a morning peak in the HO_x mixing ratio (Salawitch *et al.*, 1994; Wennberg *et al.*, 1999) that could not be explained quantitatively with model simulations. Also in the upper troposphere, a comparison of HO_x measurements with model calculations show an underestimation of the HO_x concentrations at mid-latitude for SZA $> 80°$ (Jaeglé *et al.*, 2000). Using the new recommendations, the discrepancy between the observations and the simulations might be reduced, however, more specific simulations have to be performed.

6. Conclusions

The impact of accurate calculations of photolysis frequencies on stratospheric chemistry was investigated using the photochemical box model BRAPHO. For the calculation of the photolysis frequencies the radiative transfer model PHOTOGT is used which includes a detailed treatment of the absorption cross sections of O_2 and NO as well as the radiative transfer at large solar zenith angles. Simplified treatments of the atmospheric O_2 absorption have been shown to lead to

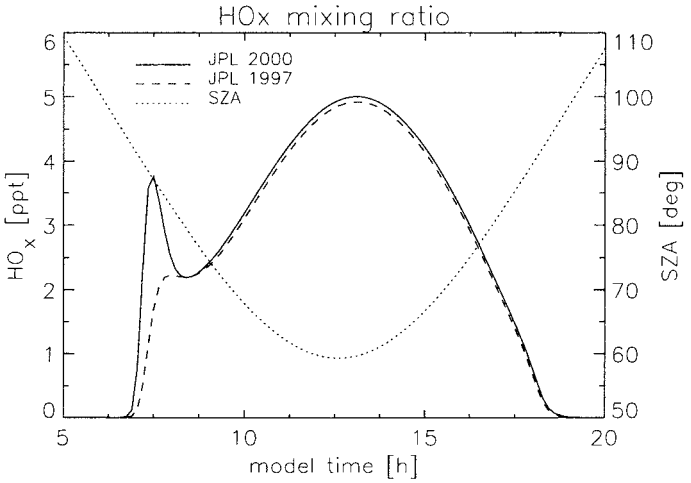

Figure 8. HO_x mixing ratio for the simulations using the old recommendation (JPL 97, Carslaw *et al.*, 1995) and the 2 updated bromine reaction rates (JPL 2000). The dotted line represents the SZA (right scale).

significant differences in $J(O_2)$ (10% for overhead sun). For J(NO) the discrepancies introduced by simplified parameterizations easily reach 100%. Refraction has been shown to increase stratospheric photolysis frequencies at visible wavelengths at large SZA by up to 100%. This enhancement leads to significant changes in twilight concentrations of several species and, under certain situations, to significant changes in nighttime concentrations of some trace gases, e.g., an decrease in the NO_3 mixing ratio by a factor of 2. Higher HOBr cross sections and a faster heterogeneous hydrolysis of bromine nitrate in the latest JPL evaluation (Sander *et al.*, 2000) compared to the previous evaluation lead to a significant increase in the simulated concentrations of BrO at mid-latitudes. Additionally, a morning maximum in the HO_x mixing ratio, also observed in measurements, is simulated using the data from the new evaluation.

Overall, the importance of the accurate calculation of the photolysis frequencies for the simulation of stratospheric chemistry has been highlighted. For the examination of the impact of special processes for stratospheric chemistry a flexible model with detailed treatment of all the main processes (gas phase reactions, photolysis reactions, heterogeneous reactions) is required. The modular structure and the detailed treatment of all known processes in stratospheric chemistry make BRAPHO an ideal tool to study stratospheric processes.

Acknowledgements

We would like to thank Glen Carver, Centre for Atmospheric Science, Cambridge University, U.K., for providing the ASAD code, Ken Carslaw, now at School of the Environment, University Leeds, U.K., for providing us the heterogeneous

chemistry tool. Jens-Uwe Grooß, now at FZ Jülich, Germany, for providing model results for comparison. Kenneth Minschwaner, Department of Physics, New Mexico Tech., U.S.A., for providing the NO absorption cross sections. This work was funded by the State and University of Bremen, the German Space Agency (DLR) and the European Union.

References

Allen, M. and Frederick, J. E., 1982: Effective photodissociation cross sections for molecular oxygen and nitric oxide in the Schumann–Runge bands, *J. Atmos. Sci.* **39**, 2066–2075.

Atkinson, R., Baulch, D. L., Cox, R. A., Hampson Jr., R. F., Kerr, J. A., Rossi, M. J., and Troe, J., 1997: Evaluated kinetic and photochemical data for atmospheric chemistry, Supplement V, *J. Phys. Chem. Ref. Data* **26** (3), 521–1011. IUPAC Subcommittee in Gas Kinetic Data Evaluation for Atmospheric Chemistry.

Balluch, M. and Lary, D. J., 1997: Refraction and atmospheric photochemistry, *J. Geophys. Res.* **102** (D7), 8845–8854.

Becker, G., Grooß, J.-U., McKenna, D. S., and Müller, R., 2000a: Stratospheric photolysis frequencies: Impact of an improved numerical solution of the radiative transfer equation, *J. Atmos. Chem.* **37**, 217–229.

Becker, G., Müller, R., McKenna, D. S., Rex, M., Carslaw, K. S., and Oelhaf, H., 2000b: Ozone loss rates in the Arctic stratosphere in the winter 1994/1995: Model simulations underestimate results of the Match analysis, *J. Geophys. Res.* **105** (D12), 15175–15184.

Blindauer, C., Rozanov, V., and Burrows, J. P., 1996: Actinic flux and photolysis frequency comparison computations using the model PHOTOGT, *J. Atmos. Chem.* **24**, 1–21.

Brown, P. N., Byrne, G. D., and Hindmarsh, A. C., 1989: VODE: A variable-coefficient ODE solver, *SIAM J. Sci. Stat. Comput.* **10** (5), 1038–1051.

Buchwitz, M., Rozanov, V. V., and Burrows, J. P., 2000: A correlated-k distribution scheme for overlapping gases suitable for retrieval of atmospheric constituents from moderate resolution radiance measurements in the visible/near-infrared spectral region, *J. Geophys. Res.* **105** (D15), 15247–15261.

Carslaw, K., Luo, B., and Peter, T., 1995: An analytic expression for the composition of aqueous HNO_3-H_2SO_4 stratospheric aerosols including gas phase removal of HNO_3, *Geophys. Res. Lett.* **22**, 1877–1880.

Carver, G. D., Brown, P., and Wild, O., 1997: The ASAD atmospheric chemistry integration package and chemical reaction database, *Computer Physics Communications* **105**, 197–215.

Chipperfield, M. P., 1999: Multiannual simulations with a three-dimensional chemical transport model, *J. Geophys. Res.* **104** (D1), 1781–1805.

Crutzen, P., Müller, R., Brühl, C., and Peter, T., 1992: On the potential importance of the gas phase reaction $CH_3O_2 + ClO \rightarrow ClOO + CH_3O$ and the heterogeneous reaction $HOCl + HCl \rightarrow H_2O + Cl_2$ in the 'ozone hole' chemistry, *Geophys. Res. Lett.* **19**, 1113–1116.

Dahlback, A. and Stamnes, K., 1991: A new spherical model for computing the radiation field available for photolysis and heating at twilight, *Planetary and Space Science* **39** (5), 671–683.

DeMajistre, R., Anderson, D., Lloyd, S., Swaminathan, P., and Zasadil, S., 1995: Effects of refraction on photochemical calculations, *J. Geophys. Res.* **100** (D9), 18817–18822.

DeMore, W. B., Sander, S. P., Golden, D. M., Hampson, R. F., Kurylo, M. J., Howard, C. J., Ravishankara, A. R., Kolb, C. E., and Molina, M. J., 1997: *Chemical Kinetics and Photochemical Data for Use in Stratospheric Modeling, Evaluation 12*, NASA JPL Pub. 97-4.

Eichmann, K.-U., 1995: Optimierung und Validierung des pseudo–sphärischen Strahlungstransportmodells GOMETRAN, Master's Thesis, Universität Bremen.

Eyring, V., 1999: Modellstudien zur arktischen stratosphärischen Chemie im Vergleich mit Meßdaten, PhD Thesis, University of Bremen.

Grooß, J.-U., Müller, R., Becker, G., McKenna, D. S., and Crutzen, P. J., 1999: The upper stratospheric ozone budget: An update of calculations based on HALOE data, *J. Atmos. Chem.* **34**, 171–183.

Grooß, J.-U., Pierce, R. B., Crutzen, P. J., Grose, W. L., and Russell III, J. M., 1997: Re-formation of chlorine reservoirs in the southern hemisphere polar spring, *J. Geophys. Res.* **102** (D11), 13141–13152.

Hansen, G., Svenøe, T., Chipperfield, M. P., Dahlback, A., and Hoppe, U.-P., 1997: Evidence of substantial ozone depletion in winter 1995/96 over Northern Norway, *Geophys. Res. Lett.* **24** (7), 799–802.

Hanson, D. and Mauersberger, K., 1988: Laboratory studies of the nitric acid trihydrate: Implications for the south polar stratosphere, *Geophys. Res. Lett.* **15** (8), 855–858.

Hanson, D., Ravishankara, A., and Solomon, S., 1994: Heterogeneous reactions in sulfuric acid aerosols: A framework for model calculations, *J. Geophys. Res.* **99**, 3615–3629.

Ingham, T., Bauer, D., Landgraf, J., and Crowley, J. N., 1998: Ultraviolet-visible absorption cross sections of gaseous HOBr, *J. Phys. Chem. A* **102** (19), 3293–3298.

Jaeglé, L., Jacob, D. J., Brune, W. H., Faloona, I., Tan, D., Heikes, B. G., Kondo, Y., Sachse, G. W., Anderson, B., Gregory, G. L., Singh, H. B., Pueschel, R., Ferry, G., Blake, D. R., and Shetter, R. E., 2000: Photochemistry of HO_x in the upper troposphere at northern midlatitudes, *J. Geophys. Res.* **105** (D3), 3877–3892.

Koop, T., Biermann, U. M., Raber, W., Luo, B. P., Crutzen, P. J., and Peter, T., 1995: Do stratospheric aerosol droplets freeze above the ice frost point?, *Geophys. Res. Lett.* **22** (8), 917–920.

Koppers, G. A. and Murtagh, D. P., 1996: Model studies of the influence of O_2 photodissociation parametrisation in the Schumann–Runge bands on ozone related photolysis in the upper atmosphere, *Annales Geophysicae* **14**, 68–79.

Krämer, M., Müller, R., Bovensmann, H., Burrows, J. P., Brinkmann, J., Röth, E.-P., Grooß, J.-U., Müller, R., Woyke, T., Ruhnke, R., Günther, G., Hendricks, J., Lippert, E., Carslaw, K. S., Peter, T., Ziegler, A., Brühl, C., Steil, B., Lehmann, R., and McKenna, D. S., 2002: Intercomparison of stratospheric chemistry models under polar vortex conditions, *J. Atmos. Chem.*, accepted.

Lary, D. and Pyle, J., 1991: Diffuse radiation, twilight, and photochemistry – I, *J. Atmos. Chem.* **13**, 373–392.

Madronich, S., 1987: Photodissociation in the atmosphere, 1. Actinic flux and effects of ground reflections and clouds, *J. Geophys. Res.* **92**, 9740–9752.

Minschwaner, K., Anderson, G. P., Hall, L. A., and Yoshino, K., 1992: Polynominal coefficients for calculating O_2 Schumann–Runge cross sections at 0.5 cm^{-1} resolution, *J. Geophys. Res.* **97** (D9), 10103–10108.

Minschwaner, K., Salawitch, R. J., and McElroy, M. B., 1993: Absorption of solar radiation by O_2: Implications for O_3 and lifetime of N_2O, $CFCl_3$, and CF_2Cl_2, *J. Geophys. Res.* **98** (D6), 10543–10561.

Minschwaner, K. and Siskind, D. E., 1993: A new calculation of nitric oxide photolysis in the stratosphere, mesosphere, and lower thermosphere, *J. Geophys. Res.* **98** (D11), 20,401–20,412.

Müller, R. W., Bovensmann, H., Kaiser, J. W., Richter, A., Rozanov, A., Wittrock, F., and Burrows, J. P., 2002: Consistent interpretation of ground based and GOME BrO SCD data, *Adv. Space Res.* **29** (11), 1655–1660.

Nevison, C. D., Solomon, S., and Garcia, R. R., 1997: Model overestimates of NO_y in the upper stratosphere, *Geophys. Res. Lett.* **24** (7), 803–806.

Peter, T., 1997: Microphysics and heterogeneous chemistry of polar stratospheric clouds, *Annu. Rev. Phys. Chem.* **48**, 785–822.

Poole, L. R. and McCormick, M. C., 1988: Polar stratospheric clouds and the Antarctic ozone hole, *J. Geophys. Res.* **93**, 8423–8430.

Prather, M., 1993: I. GISS photochemical model, in M. Prather and E. Remsberg (eds), *The Atmospheric Effects of Stratospheric Aircraft: Report of the 1992 Models and Measurements Workshop*, Vol. 1292 of *NASA Reference Publication*, pp. 76–85.

Prather, M., Ehhalt, D., Dentener, F., Derwent, R., Dlugokencky, E., Holland, E., Isaksen, I., Katima, J., Kirchhoff, V., Matson, P., Midgley, P., and Wang, M., 2001: Atmospheric chemistry and greenhouse gases, in J. T. Houghton, Y. Ding, D. J. Griggs, M. Noguer, P. J. van der Linden, X. Dai, K. Maskell, and C. A. Johnson (eds), *Climate Change 2001: The Scientific Basis. Contribution of Working Group I to the Third Assessment Report of the Intergovernmental Panel on Climate Change*, Cambridge University Press, Cambridge, United Kingdom and New York, NY, U.S.A., pp. 239–288.

Press, W. H., Teukolsky, S. A., Vetterling, W. T., and Flannery, B. P., 1992: *Numerical Recipes: The Art of Scientific Computation*, Cambridge University Press, 2nd edn.

Raffalski, U., Klein, U., Franke, B., Langer, J., Sinnhuber, B.-M., Trentmann, J., Künzi, K., and Schrems, O., 1998: Ground based millimeter-wave observations of Arctic chlorine activation during winter and spring of 1996/97, *Geophys. Res. Lett.* **25** (17), 3331–3334.

Randeniya, L. K., Vohralik, P. F., Plumb, I. C., and Ryan, K. R., 1996: Heterogeneous $BrONO_2$ hydrolysis: Effect on NO_2 columns and ozone at high latitudes in summer, *J. Geophys. Res.* **102** (D19), 23543–23557.

Ravishankara, A. R., Shepherd, T. G., Chipperfield, M. P., Haynes, P. H., Kawa, S. R., Peter, T., Plumb, R. A., Portmann, R. W., Randel, W. J., Waugh, D. W., and Worsnop D. R., 1999: Lower stratospheric processes, in *Scientific Assesment of Ozone Depletion: 1998*, World Meteorological Organization, Global Ozone Research and Monitoring Project – Report No. 44, pp. 7.1–7.76.

Renard, J.-B., Pirre, M., Robert, C., Moreau, G., Huguenin, D., and Russell III, J., 1996: Nocturnal vertical distribution of stratospheric O_3, NO_2, and NO_3 from baloon measurements, *J. Geophys. Res.* **101**, 28793–28804.

Rozanov, V. V., Diebel, D., Spurr, R. J. D., and Burrows, J. P., 1997: GOMETRAN: A radiative transfer model for the satellite project GOME – The plane-parallel version, *J. Geophys. Res.* **102** (D14), 16683.

Salawitch, R. J., Wofsy, S. C., Wennberg, P. O., Cohen, R. C., Anderson, J. G., Fahey, D. W., Gao, R. S., Keim, E. R., Woodbridge, E. L., Stimpfle, R. M., Koplow, J. P., Kohn, D. W., Wbster, C. R., May, R. D., Pfister, L., Gottlied, E. W., Michelsen, H. A., Yue, G. K., Prather, M. J., Wilson, J. C., Brock, C. A., Jonsson, H. H., Dye, J. E., Baumgardner, D., Proffitt, M. H., Loewenstein, M., Podolske, J. R., Elkins, J. W., Dutton, G. S., Hintsa, E. J., Dessler, A. E., Weinstock, E. M., Kelly, K. K., Boering, K. A., Daube, B. C., Chan, K. R., and Bowen, S. W., 1994: The diurnal variation of hydrogen, nitrogen, and chlorine radicals: Implications for the heterogeneous production of HNO_2, *Geophys. Res. Lett.* **21** (23), 2551–2554.

Sander, S. P., Friedl, R. R., DeMore, W. B., Ravishankara, A. R., Golden, D. M., Kolb, C. E., Kurylo, M. J., Hampson, R. F., Huie, R. E., Molina, M. J., and Moortgat: G. K., 2000: *Chemical Kinetics and Photochemical Data for Use in Stratospheric Modeling, Evaluation 13, Supplement to Evaluation 12: Update of Key Reactions*, NASA JPL Pub. 00-3, available at http://jpldataeval.jpl.nasa.gov/.

Sinnhuber, B.-M., Müller, R., Langer, J., Bovensmann, H., Eyring, V., Klein, U., Trentmann, J., Burrows, J., and Künzi, K., 1999: Interpretation of mid-stratospheric arctic ozone measurements using a photochemical box-model, *J. Atmos. Chem.* **34**, 281–290.

Siskind, D. E., Minschwaner, K., and Eckman, R. S., 1994: Photodissociation of O_2 and H_2O in the middle atmosphere: Comparison of numerical methods and impact on model O_3 and OH, *Geophys. Res. Lett.* **21** (10), 863–866.

Stolarski, R. S., 1995: *1995 Scientific Assessment of the Atmospheric Effects of Stratospheric Aircraft*, NASA Reference Publication 1381.

Tabazadeh, A., Turco, R., Drdla, K., Jacobson, M., and Toon, O., 1994: A study of Type I polar stratospheric cloud formation, *J. Geophys. Res.* **21** (15), 1619–1622.

Wennberg, P. O., Salawitch, R. J., Donaldson, D. J., Hanisco, T. F., Lanzendorf, E. J., Perkins, K. K., Lloyd, S. A., Vaida, V., Gao, R. S., Hintsa, E. J., Cohen, R. C., Swartz, W. H., Kusterer, T. L., and Anderson, D. E., 1999: Twilight observations suggest unknown sources of HO_x, *Geophys. Res. Lett.* **26** (10), 1373–1376.

Wittrock, F., Müller, R., Richter, A., Bovensmann, H., and Burrows, J., 2000: Measurements of iodine monoxide (IO) above Spitsbergen, *Geophys. Res. Lett.* **27** (10), 1471–1474.

WMO, 1985: *Atmospheric Ozone*, World Meteorological Organization, Global Ozone Research and Monitoring Project, Report No. 16.

Woyke, T., Müller, R., Stroh, F., McKenna, D., Engel, A., Margitan, J. J., Rex, M., and Carslaw, K. S., 1999: A test of our understanding of the ozone chemistry in the Artic polar vortex based on in situ measurements of ClO, BrO, and O_3 in the 1994/1995 winter, *J. Geophys. Res.* **104** (D15), 18755–18768.

Yoshino, K., Cheung, A. S.-C., Esmond, J. R., Parkinson, W. H., Freeman, D. E., Jenouvier, A., Coquart, B., and Merienne, M. F., 1988: Improved absorption cross-sections of oxygen in the wavelength region 205–240 nm of the Herzberg Continuum, *Planetary and Space Science* **36** (12), 1469–1475.